



Efficient Out-of-Distribution Detection with Prototypical Semi-Supervised Learning and Foundation Models

Evelyn Mannix¹  and Howard Bondell² 

¹ Melbourne Centre for Data Science
University of Melbourne
Melbourne, Australia 3010
`evelyn.mannix@unimelb.edu.au`

² Melbourne Centre for Data Science
University of Melbourne
Melbourne, Australia 3010
`howard.bondell@unimelb.edu.au`

Abstract. This paper describes PAWS-VMK, an improved approach to prototypical semi-supervised learning in the field of computer vision, specifically designed to utilize a frozen foundation model as the neural network backbone. This method outperforms previous results in semi-supervised learning and out-of-distribution (OOD) detection, improving upon the **P**redicting **V**iew-**A**ssignments **W**ith **S**upport **S**amples (PAWS) semi-supervised learning method. We introduce (1) parametric von-Mises Fisher Stochastic Neighbour Embedding (**vMF-SNE**) to pretrain the projection head using the high-quality embeddings of the foundation model; (2) a **MixMatch** inspired loss, where predictions across multiple views are averaged to provide a more reliable supervision signal compared to the consistency loss used in PAWS and (3) simple k -Means prototype selection (**SKMPS**), a technique that provides superior performance to other unsupervised label selection approaches in this context. PAWS-VMK sets new benchmarks in semi-supervised learning for CIFAR-10 (99.2%) and CIFAR-100 (89.8%) with four labelled instances per class, and Food-101 (90.1%) with two labelled instances per class. We also observe that PAWS-VMK can efficiently detect OOD samples in a manner that is competitive with specialised methods specifically designed for this purpose, achieving 93.1/98.0 and 95.2/96.3 on the CIFAR-10 and CIFAR-100 OpenOOD benchmarks.

Keywords: prototypical deep-learning · semi-supervised learning · out-of-distribution detection · foundation models · image classification

1 Introduction

From managing weeds [1], to food safety [2], to diagnosing cancer [3], deep learning is used extensively in computer vision applications where specialised

knowledge is needed to annotate data. Within these contexts, identifying out-of-distribution (OOD) data, such as plants or food contaminants not present in the training dataset, can also be of great importance. This creates a need for semi-supervised learning (SSL) approaches that can learn accurate models with only a small number of annotations, and that also perform well on detecting OOD examples. While SSL [4,5] and OOD detection [6,7] methods are well developed, few studies consider them simultaneously.

Prototype deep learning approaches, which learn a metric or semi-metric space for classifying items based on their proximity to class prototypes, present a promising solution for this challenge. Prototypical approaches have been previously used in semi-supervised learning [8] and OOD detection [9,10]. They have also been applied in various other contexts such as improving OOD generalisation [11], robust classification [12], few-shot learning [13] and in multi-modal applications [14].

Central to recent advances in prototypical methods is self-supervised learning [8–10]. Self-supervised techniques use pretext tasks defined by the data to create a supervisory signal, such as in SimCLR [15] where models are trained to identify pairs of augmented views of an image. This creates a feature space where images with similar semantic information are grouped together, and the foundation methods trained on large datasets using these techniques show promising generalizability across multiple image domains [14,16,17]. Leveraging these foundation models is a promising direction for both prototypical and semi-supervised approaches to improve performance as well as training efficiency.

In this paper we introduce PAWS-VMK, a novel semi-supervised approach designed to be used with foundation models that sets new benchmarks in SSL and OOD detection. This method improves upon the **P**redicting **V**iew-**A**ssignments **W**ith **S**upport **S**amples (PAWS) SSL approach [8] by exploring how it can be effectively trained using a foundation model as a backbone. We identify three challenges with the original approach and in each case propose solutions to improve performance

1. Randomly initializing the projection head, which is used after the neural network backbone to make predictions in PAWS, can result in poor performance for some datasets. We propose parametric vMF-SNE pretraining to solve this problem.
2. The consistency loss used in PAWS can degrade model performance over a training run. We introduce a MixMatch [18] inspired loss that can train more accurate models.
3. Randomly selecting prototype images for the labelled dataset, even when stratifying by class, can result in poor performance. We propose the simple k -means prototype selection (SKMPS) strategy, that outperforms other state-of-the-art unsupervised label selection methods in this context.

2 Related work

Foundation models. In computer vision, foundation models are used as functional maps from the image domain to a representation space that captures the semantic content of the image with minimal loss of information. The degree to which semantic content is retained can be tested by undertaking downstream tasks within the representation space, such as image classification, segmentation and object detection [19]. Current state-of-the-art foundation models include methods that combine several self-supervised approaches on large datasets, such as DINOv2 [17], and other approaches that use language-image pretraining approaches such as CLIP [14, 20].

Semi-supervised learning. In semi-supervised learning (SSL), a model is trained to perform a particular task, such as image classification, using a small set of labelled data and a much larger set of unlabelled data. By taking into account the distribution of the unlabelled data within the learning process, SSL methods can train more accurate models compared to approaches that only utilize the labelled data within this context [5]. The earliest SSL approaches used pseudolabelling [21], and a number of modern approaches have extended on this idea such as FixMatch [22], which employs image augmentation to efficiently propagate labels, and other similar methods [23–25].

Out-of-distribution detection. The problem of out-of-distribution (OOD) detection in deep learning was introduced when it was observed that neural networks tend to provide overconfident results when making predictions on images with previously unseen classes or that are unrecognizable [26]. OOD detection methods are designed to detect when inference is going to be made on such data, so an appropriate alternative action can be taken [27]. Various OOD detection approaches have been proposed [7, 28–30], including several methods that use a prototypical approach to create embeddings in which the in-distribution images are tightly clustered [9, 10]. Most OOD detection methods assume class labels are available for all images, and few have considered the entirely unsupervised case [10].

Stochastic Neighbour Embedding. Given a high dimensional dataset, Stochastic Neighbour Embedding (SNE) [31] methods create a representation of this data in a smaller dimensional space while attempting to ensure the relationship between items in the dataset is preserved. They are often used for plotting high dimensional data in lower dimension spaces [32]. One of the most well-known and commonly used methods is the t-distributed Stochastic Neighbour Embedding (t-SNE) approach [33].

Prototype selection strategies. The goal of prototype selection is to choose from an unlabelled dataset an optimal set of images with which to label and

undertake semi-supervised, active or few-shot learning. Other works have referred to this challenge as unsupervised selective labelling [34], or the cold start problem [35]. The optimal image set is defined as the set of images for a given labelling budget that obtain maximal performance under a particular learning paradigm. While it has been found that using these prototypical image sets can lead to significant performance improvements [22, 24, 36], identifying them is challenging. The Unsupervised Selective Labelling (USL) [34] approach is the current state-of-the-art method for unsupervised prototype selection when using a frozen backbone, such as a foundation model or when using self-supervised learning.

3 Methodology

3.1 Preliminaries

Setup. Semi-supervised learning (SSL) aims to train a model using a small labelled dataset $D_l := \{x_l, y_l\}$ and a much larger unlabelled dataset $D_u := \{x_u\}$. In this paper, we are interested in image classification using frozen foundation models as the backbone of the network. The foundation model maps the data onto a representational space, as defined by a neural network $f_\theta : X \in \mathbb{R}^{3 \times H \times W} \rightarrow Z \in \mathbb{R}^{d_1}$. Here H and W are the height and width of the input images X , and d_1 is the dimensionality of this representation space. This representation space Z can also be referred to as a latent space.

Predicting View Assignments With Support Samples. PAWS [8] is a prototypical SSL method that takes inspiration from self-supervised learning approaches. PAWS adapts the idea of prototypes from **Swapping Assignments Between Multiple Views** (SwAV) [37], which learns prototype vectors to cluster data for self-supervised learning. However, PAWS uses embeddings of the labelled images D_l as prototypes instead of learning them non-parametrically.

Architecture. PAWS [8] uses an architecture with a backbone f_θ and a projection head, defined by a second neural network $g_\phi : Z \in \mathbb{R}^{d_1} \rightarrow \hat{Z} \in \mathbb{R}^{d_2}$. This creates a second latent space \hat{Z} with dimension d_2 , which depending on the problem may be smaller or larger than d_1 . Projection heads are often used in self-supervised learning [38].

Similarity kernel and predictions. Following [39], PAWS can be written down as a generative model. The probability density of a sample from the dataset is defined using the prototypes from the labelled dataset D_l and a similarity kernel,

$$p(x_j | D_l) := \frac{1}{|D_l|} \sum_{x_i \in D_l} k_{\hat{Z}}(x_j; x_i) \quad (1)$$

where the similarity kernel is defined by

$$k_{\hat{z}}(x_j; x_i) := C_z \exp(\hat{z}_j \cdot \hat{z}_i / \tau) \quad (2)$$

$$\hat{z} := \frac{g_\phi(z)}{\|g_\phi(z)\|}, \quad z := f_\theta(x) \quad (3)$$

with C_z a normalizing constant. PAWS defines this conditional probability within the second latent space \hat{Z} , employing the projection head g_ϕ .

For a particular class y , we can use the set of prototypes that belong to a class, $B_y = \{x_i, y_i\} \in D_l | y_i = y\}$, to define the support of an image conditional on the class y

$$p(x_j | y, D_l) := \frac{1}{|B_y|} \sum_{x_i \in B_y} k_{\hat{z}}(x_j; x_i) \quad (4)$$

and through Bayes' rule, we can derive the predicted class probabilities as

$$p(y | x_j, D_l) = \frac{p(x_j | y, D_l) p(y)}{p(x_j | D_l)} \quad (5)$$

$$= \sigma(\hat{z}_j \cdot \hat{z}_S^T / \tau) y_S = p_j \quad (6)$$

where y_S is the one-hot encoded or soft labels corresponding to the classes of the prototypes, τ is a temperature hyperparameter and σ is the softmax function. Finally, z_S is the matrix of latent representations of the prototypes. The last step assumes class balance in the data and prototypes, setting $p(y) = \frac{1}{C}$ and $B_y = N/C$ where C is the total number of classes in the dataset.

Training objective. PAWS uses a consistency loss as a supervision signal, employing cross-entropy to encourage the prediction of two views of the same image to be similar. The loss is given by

$$L_{paws} := \frac{1}{2n} \sum_{i=1}^n (H(\rho(p_i^+), p_i) + H(\rho(p_i), p_i^+)) - H(\bar{p}) \quad (7)$$

where p_i and p_i^+ are the probabilities given by Eq. (6) for different augmented views of an image, n is the number of unlabelled images and ρ is a sharpening function used to prevent representation collapse as will be discussed in Sec. 3.2. In the final term, \bar{p} is the average of the sharpened predictions on the unlabelled images. This mean entropy maximization regularization (me-max) term is used to maximise the entropy of the average predictions [8]. This helps ensure that the association of the unlabelled points with each class is more uniform. An overview of the PAWS training framework is shown in Fig. 1b.

3.2 Improving the PAWS approach

Our goal is to adapt the PAWS semi-supervised learning approach to perform well with a foundation model, and obtain better OOD detection results. To

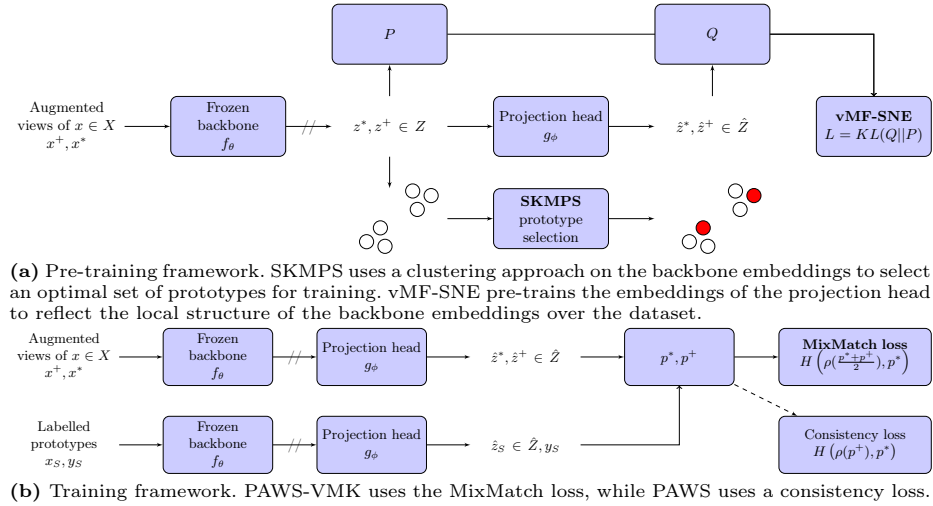


Fig. 1: Overview of our proposed framework for PAWS-VMK.

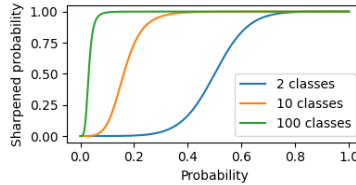


Fig. 2: Impact of sharpening approach in PAWS on the class probability. The horizontal axis describes probability of the first class, and vertical axis describes the sharpened probability when $T = 0.25$ in Equation 8, with the probability of all other classes set to be equal in the input.

achieve this we propose PAWS-VMK, which incorporates a MixMatch loss, a vMF-SNE pretraining strategy, and the SKMPS strategy for selecting optimal prototypes. An overview of these components is provided in Fig. 1.

Sharpening and MixMatch loss. The consistency loss employed by PAWS in Eq. (7) penalises the prediction from one augmented view of an image differing from another. However, a sharpening function ρ is used within this loss to prevent representational collapse and encourage confident predictions,

$$\rho(p)_i := \frac{p_i^{1/T}}{\sum_{i=1}^C p_i^{1/T}} \quad (8)$$

with the temperature parameter T fixed at $T = 0.25$ [8]. Fig. 2 shows that for moderately confident predictions, this level of sharpening quickly leads to an entirely confident sharpened prediction, particularly with a large number of

classes. If a particular image is augmented such that each view is sharpened to a confident prediction of a different class, this will cause undesirable *mixing* at the class boundaries, and we observe performance degradation over a training run when this loss is used with frozen DINOv2 embeddings (Fig. S1).

Instead we propose to use a MixMatch [18] inspired loss, that averages the predictions from multiple views before sharpening to provide a more consistent supervision signal and improve accuracy. The PAWS approach uses two global views within the consistency loss, and we propose to jointly sharpen the two global views together to create the MixMatch loss

$$L_{\text{MixMatch}} := \frac{1}{2n} \sum_{i=1}^n \left(H \left(\rho \left(\frac{p_1 + p_2}{2} \right), p_i \right) + H \left(\rho \left(\frac{p_1 + p_2}{2} \right), p_i^+ \right) \right) - H(\bar{p}). \quad (9)$$

Pretraining with vMF-SNE. If we are using a pretrained backbone model f_θ , which provides a *good* representation of our data in the first latent space Z , a *good* starting point for our projection head g_ϕ should reflect the local structure of the first latent space Z within the second \hat{Z} . This is not a given if we randomly initialize the parameters of the projection head, and without placing restrictions on its architecture and the dimensionality of our latent spaces, we cannot simply initialise it as an identity mapping.

A potential solution is to pretrain our projection head using a parametric Stochastic Neighbour Embedding (SNE) approach [31]. This method involves building two probability distributions that describe the similarity of data points in two different spaces, the origin space P and the target space Q . The idea is for similar points i, j in P to have a high probability p_{ij} compared to dissimilar points, and to fit the distribution in the target space Q to the distribution in the origin space P by minimizing the KL divergence

$$\text{KL}(Q||P) = \sum_{ij} p_{ij} \log \frac{p_{ij}}{q_{ij}} \quad (10)$$

where p_{ij} and q_{ij} describe the similarity between points in the origin and target space.

These P, Q distributions are built using a probability distribution as a kernel. Taking inspiration from the probabilistic perspective of PAWS [39], we propose to use a von-Mises Fisher (vMF) distribution [40] in the origin and target spaces. This is the same as the PAWS similarity kernel in Eq. (2) with the normalizing constant given by $C_z = C_p(1/\tau)$, with $1/\tau$ the concentration parameter. The normalization constant C_p is expensive to compute, but can be efficiently approximated [41].

Using the vMF kernel to compute the probabilities P in the latent space defined by our backbone model Z , we have

$$p_{j|i} := \frac{k_Z(x_j; x_i)}{\sum_{k \neq i} k_Z(x_k; x_i)}, \quad (11)$$

$$k_Z(x_j; x_i) := C_p(\kappa_i) \exp(z'_j \cdot z'_i \kappa_i), \quad (12)$$

$$z' := \frac{f_\theta(x)}{\|f_\theta(x)\|} \quad (13)$$

$$(14)$$

where we define $p_{i|i} = 0$, and note that the normalization constant cancels out in this expression. We set κ_i for each point to make the entropy H_i equal to the perplexity parameter γ , $H_i = \sum_k p_{k|i} \log p_{k|i} = \gamma$. This ensures each point has a similar number of neighbours in the distribution P , and for each point κ_i is determined using the bisection method. To obtain a symmetric distribution, we use $p_{ij} = \frac{p_{j|i} + p_{i|j}}{2N}$, where N is the number of data points.

To compute the probability distribution Q of the second latent space \hat{Z} , a vMF distribution with fixed concentration is used as the kernel,

$$q_{j|i} = \frac{k_{\hat{Z}}(x_j; x_i)}{\sum_{k \neq i} k_{\hat{Z}}(x_k; x_i)} \quad (15)$$

where k_{Z_2} is the PAWS kernel (Eq. (2)) and we define $q_{i|i} = 0$. We also symmetrise this conditional distribution as above to obtain q_{ij} .

To minimize the KL divergence in Eq. (10), gradients are taken with respect to the parameters of the projection head g_ϕ . This allows the vMF-SNE pre-training to follow a similar approach as to training the neural networks in PAWS, utilising mini-batching, stochastic gradient descent and image augmentations [8].

This parametric vMF-SNE pretraining method is similar to t -SNE [33], parametric t -SNE [42] and non-parametric vMF-SNE [43], but we apply it in a very different context — as a self-supervised approach for pre-training a neural network using a frozen foundation model. There are three key hyper-parameters in this process — the batch size, which defines the number of images to sample in each mini-batch, the perplexity parameter γ , and the concentration of the vMF distributions in Z_2 which is determined by τ . An ablation study considering the impact of these parameters is presented in the supplementary material.

Prototype selection. In this work we propose the simple k -means prototype selection (SKMPS) strategy. This approach provides for a diverse sampling of prototypes in three steps

1. Calculate normalized embeddings using a foundation model — z' in Eq. (14).
2. Cluster the data into k clusters. We set k to be the number of images (budget) desired for the labelled dataset D_l .
3. Select the image closest to the centroid of each cluster as a prototype.

We choose k -means clustering [44] for the clustering algorithm in the second step as it is fast to compute and allows for the selection of a fixed number of clusters. The k -means algorithm minimises the sum of squared euclidean distances to the cluster centroids [44]. By normalizing the image embeddings given by the foundation model in the first step, the squared euclidean distance becomes proportional to cosine distance, which can be used for determining image similarity with foundation models [14, 17]. In this sense, the SKMPS procedure can be interpreted as identifying clusters of visually similar images, and selecting the most representative image from each cluster as a prototype.

4 Experiments

4.1 Implementation details

We closely follow the implementation of PAWS [8] for our experiments, but are able to shorten the training regime as we freeze the weights of the DINOv2 foundation models that are used for the model backbone. All of the semi-supervised learning models that are fitted in this paper were trained for 50 epochs, and the vMF-SNE pretraining runs were trained for 20 epochs. This meant that even for the Food-101 dataset with 75,000 images, training a single model took less than two hours with two Nvidia V100 32GB graphics cards for the ViT-S/14 and ViT-B/14 backbone, and around six hours for the ViT-L/14 backbone. In contrast to the original PAWS approach [8], we only use the projection head as a classifier, using the inference formula in Eq. (6) to make predictions using the labelled prototypes. Further details and hyperparameters are provided in the supplementary material.

4.2 Datasets

Seven datasets were selected to demonstrate our approach. These include CIFAR-10 (10 classes), CIFAR-100 (100 classes) [45], EuroSAT (10 classes) [46], Flowers-102 (102 classes) [47], Food-101 (101 classes) [48], Oxford Pets (37 classes) [49] and DeepWeeds (2 classes) [1]. While DeepWeeds has originally 9 classes, we treat it as a binary classification problem to identify weeds versus not weeds, due to the size of the negative class.

When sampling the prototypes for semi-supervised learning, we selected 4 (CIFAR-10), 4 (CIFAR-100), 4 (EuroSAT), 27 (DeepWeeds - binary), 2 (Flowers-102), 2 (Food-101) and 2 (Oxford Pets) images per class. Results are reported as the mean of five runs and the standard deviation, with the same sets of prototypes being used for all experiments unless specified otherwise, where the USL [34] or SKMPS strategy is used to select prototypes. For EuroSAT and DeepWeeds, where preset validation splits were not available, we sampled 500 images per class, and 30% of the images for the 9 original classes respectively.

For the OOD detection experiments, we follow the OpenOOD [7] benchmark in choosing comparable datasets that are similar (near OOD) to CIFAR-10 and

Table 1: Performance of PAWS-VMK versus PAWS and other methods. Comparable model sizes in each column are underlined, and the best performing model of these is **bolded**. Entries noted with * use a larger labelled dataset (1% of the data) than in our benchmarks.

Methods	Backbone		Datasets		
			C10	C100	Food
FreeMatch [55]	WRN-28-2	1M	<u>95.1</u>		
+SemiReward [23]	ViT-S-P4-32	21M		84.4	
Semi-ViT [25]	ViT-Base	86M			<u>82.1</u> *
PAWS [8]	DINOv2 ViT-S/14 (f)	21M	<u>92.9</u> ±2.1	70.9±1.5	75.1±2.0
PAWS-VMK	DINOv2 ViT-S/14 (f)	21M	95.9 ±0.0	77.3±0.4	81.7±0.7
	DINOv2 ViT-B/14 (f)	86M	98.1±0.1	85.5±0.3	87.2 ±0.8
	DINOv2 ViT-L/14 (f)	300M	99.2±0.0	89.8±0.2	90.1±0.8

CIFAR-100, which include each other respectively and the Tiny ImageNet [50] dataset. We also explore the dissimilar (far OOD) benchmark for these datasets, which include Places365 [51], DTD [52], MNIST [53] and SVHN [54].

4.3 Main results

PAWS-VMK is competitive with previous semi-supervised methods.

Tab. 1 shows that across a range of benchmarking datasets our method outperforms PAWS using the same frozen backbone model, and is competitive with other methods in the literature that train models of similar sizes and using the same number (or greater) of labelled images. We outperform FreeMatch [24] on CIFAR-10 by 0.8% on average with the smallest DINOv2 model available, and also outperform Semi-ViT [23] by 5.1% using a much smaller labelled set. SemiReward [23] obtains better results with a similar model size for CIFAR-100, but in contrast to our approach they fit all model parameters whereas we use a frozen backbone. We outperform SemiReward (+1.1%) with the ViT-B model, which takes about four hours of GPU time using Nvidia V100 GPUs, compared to the 67 hours of compute time for SemiReward on a more powerful Nvidia A100 GPU [23].

PAWS-VMK is competitive with previous OOD detection methods.

Tab. 2 shows that our method performs similarly to specialised OOD detection methods for CIFAR-10, and outperforms them by a large margin for CIFAR-100, using the DINOv2 ViT-S/14 frozen backbone. We use the maximum cosine similarity to a labelled prototype as the OOD metric for the PAWS and PAWS-VMK embeddings. One the strengths of our approach is that the in-distribution embeddings are designed to cluster around a small set of prototypes, which makes OOD evaluation much more efficient than other metrics such as KNN [28], which

Table 2: Out of distribution detection results on the OpenOOD benchmark [7]. This benchmark reports the average AUROC is reported across the Near-OOD and Far-OOD datasets. The best performing models are **bolded**.

Methods		Datasets			
		CIFAR-10		CIFAR-100	
		Near-OOD	Far-OOD	Near-OOD	Far-OOD
Supervised	DeepEnsemble [7, 29]	90.6	93.2	82.7	80.7
	KNN [7, 28]	90.5	92.8	79.9	82.2
	CIDER [9, 10]	90.7	94.7	72.1	80.5
	LogitNorm [7, 30]	92.5	96.7	78.4	81.3
	PixMix [7, 56]	93.1	95.7	79.6	85.5
	PALM [10]	93.0	98.1	76.9	93.0
Semi-supervised	PAWS [8]	82.6	90.5	90.6	94.5
	PAWS-VMK	93.1	98.0	95.2	96.3

Table 3: Performance improvements from vMF-SNE pretraining and MixMatch loss across a wider range of datasets. Our method is called PAWS-VM here as it does not include the simple k -means prototype selection (SKMPS) strategy. The best performing models are **bolded**.

Method	Components			Datasets						
	Head init.	Loss type	Label selection	C10	C100	EuroSAT	DeepWeeds	Flowers	Food	Pets
PAWS [8]	Random init.	consistency	Random stratified	92.9±2.1	70.9±1.5	94.4±0.3	72.6±4.5	98.5±0.7	75.1±2.0	90.2±1.0
PAWS-VM vMF-SNE	MixMatch	Random stratified		95.8±0.1	75.7±0.9	94.2±0.1	87.8±1.5	98.9±0.6	75.9±1.8	91.6±0.2

uses a larger sample of the training dataset to determine if a new point is OOD. The other prototypical OOD approaches CIDER [9] and PALM [10] employ the KNN or Mahablonis distance [57] OOD metric to make predictions, of which the latter typically uses class information which would be unavailable in a semi-supervised setting. The PAWS-VMK projection head also provides more reliable OOD detection than the DINOv2 backbone embeddings (Tab. S2), and more detailed results for each dataset are provided in the supplementary materials.

4.4 Ablation studies

vMF-SNE pretraining and MixMatch loss provide performance benefits in combination. Fig. 3 shows that across the CIFAR-10, CIFAR-100, Food-101 and DeepWeeds datasets, these components together lead to the best overall results. For CIFAR-10 and CIFAR-100, MixMatch loss significantly improves overall accuracy and the gain from vMF-SNE pretraining is less obvious. However, for DeepWeeds skipping vMF-SNE pretraining leads to poor results. In the case of the Food-101 dataset, the combination of both vMF-SNE pretraining and MixMatch leads to be best average accuracy across all training runs.

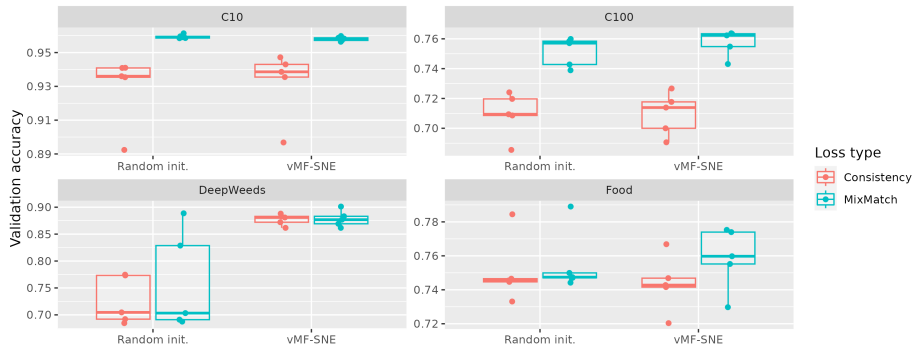


Fig. 3: Comparison of the vMF-SNE pretraining and MixMatch loss components of PAWS-M³ versus the original PAWS approach.

Table 4: Performance of different prototype selection strategies. The best performing prototype selection strategy for each dataset is **bolded**.

Method	Components			Datasets		
	Head init.	Loss type	Label selection Strat.	C10	C100	Food
PAWS	Random init.	consistency	Random Strat.	92.9±2.1	70.9±1.5	75.1±2.0
	Random init.	consistency	SKMPS	94.4±0.5	74.8±0.3	80.5±0.6
	Random init.	consistency	USL [34]	93.6±0.4	74.4±0.6	79.1±1.1
PAWS-VM	vmf-SNE	MixMatch	Random Strat.	95.8±0.1	75.7±0.9	75.9±1.8
PAWS-VMK	vmf-SNE	MixMatch	SKMPS	95.9±0.0	77.3±0.4	81.7±0.7
	vmf-SNE	MixMatch	USL [34]	95.8±0.1	77.5±0.4	80.0±1.0

In Tab. 3 the performance of these two components together in comparison to PAWS is explored across seven benchmarking datasets. Significantly better performance is observed in four of these, including CIFAR-10, CIFAR-100, DeepWeeds and Oxford Pets.

Simple k -means prototype selection (SKMPS) improves performance.

Tab. 4 shows that using prototype selection strategies improves the performance of both PAWS and PAWS-VM, and that the best performing approach across both methods and all three datasets considered is our SKMPS strategy. While the results between USL [34] and SKMPS are similar for CIFAR-100, significantly better results are obtained on the CIFAR-10 dataset using PAWS, and on the Food-101 dataset using both PAWS and PAWS-VM. SKMPS also provides more consistent results than USL for the Food-101 dataset, with a smaller variance in performance.

Table 5: Out of distribution detection results on the OpenOOD benchmark [7]. This benchmark reports the average AUROC is reported across the Near-OOD and Far-OOD datasets. The best performing models are **bolded**.

Methods	Components			Datasets		
	Head init.	Loss type	Label selection	Strat.	CIFAR-10	
PAWS [8]	Random init.	consistency	Random	Strat.	82.6	90.5
	Random init.	MixMatch	Random	Strat.	91.4	95.6
PAWS-VM	vMF-SNE	MixMatch	Random	Strat.	93.2	96.6
PAWS-VMK	vMF-SNE	MixMatch	SKMPS		93.1	98.0

Each component of PAWS-VMK improves OOD detection performance. Tab. 5 shows that MixMatch loss, vMF-SNE pretraining and Simple k -means prototype selection all contribute to improving OOD performance over the PAWS baseline. By comparing the OOD detection results for each component being introduced individually, it can be seen that MixMatch loss and vMF-SNE pretraining improve on the Near-OOD and Far-OOD benchmarks over PAWS, and that introducing the SKMPS label selection strategy results in a similar Near-OOD result but better Far-OOD detection.

5 Discussion

PAWS-VMK learns compact representations. Fig. 4 shows that our method learns a much more compact representation around the labelled prototypes in comparison to PAWS, which has been noted by the authors of CIDER [9] and PALM [10] to improve OOD detection performance. These methods use a specialised optimization loss that is designed to directly achieve this goal. While we aim to improve semi-supervised performance, the components introduced also encourage compact representations. Using a MixMatch rather than consistency based loss provides a more consistent supervision signal, as the same soft pseudo-label is applied to both augmented views of an image, encouraging more compact embeddings. The vMF-SNE pretraining approach encourages in-distribution points in the projection head embeddings to be close to other points, through the the perplexity parameter in Eq. (13). Finally, selecting a representative set of labelled prototypes using SKMPS results in them being more centralised within the in-distribution data in the final embeddings, as can be seen in Fig. 4.

vMF-SNE pretraining improves the separability of complex class representations. Fig. S2 shows that vMF-SNE pretraining helps PAWS-VMK learn better models when the backbone embeddings clusters them poorly in the first instance. Fig. 5b and Fig. 5c show the low dimensional representations of

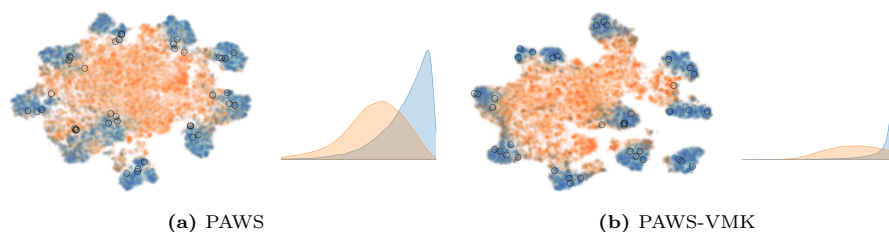


Fig. 4: t -SNE visualisation of the projection head embeddings and density plots of minimum cosine distance to a prototype (\circ) for in-distribution CIFAR-10 (blue) and OOD CIFAR-100 (orange).

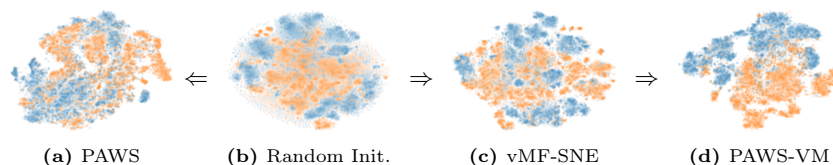


Fig. 5: t -SNE visualisation of the projection head embeddings at various stages of the training process for DeepWeeds. Blue is the weed present class, and orange is the negative class. The arrows represent the order of training steps.

the embeddings of the DINOv2 foundation model backbone on the DeepWeeds dataset, where separation of the weeds versus not weeds classes is quite poor. While training using PAWS results in mediocre performance and a mixing of the two classes (Fig. 5a), training using the vMF-SNE pretrained head results in better separation (Fig. 5d). We show in Tab. S3 in the supplementary material that this also holds in a transfer learning context.

SKMPS selects more diversity in comparison to USL. Fig. 6 shows that SKMPS samples a more diverse set of prototypes in comparison to USL. We explore this further in the supplementary material, showing in Fig. S2 that SKMPS samples more classes than USL on small budgets. For example, for 202 prototypes on the Food-101 dataset, USL never selects all of the classes in 20 runs whereas SKMPS samples all the classes in 25% of cases. The USL approach considers density to be an indicator of prototype informativeness, and preferentially chooses prototypes from denser regions of the representation space Z [34]. In contrast, SKMPS only considers the density of the points through the k -means clustering process, which results in a more diverse sample.

Compatibility with RoPAWS. The components of PAWS-VMK also provide performance benefits when used with RoPAWS [39], a PAWS based approach for semi-supervised learning with OOD data (Tab. S4).

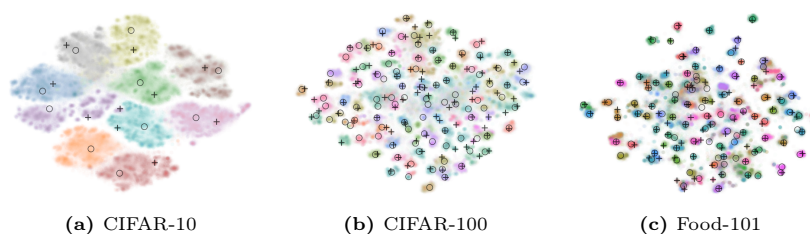


Fig. 6: *t*-SNE visualisation of the DINOv2 ViT-S/14 backbone embeddings overlaid with the prototypes selected by the USL (+) and SKMPS (o) strategies.

References

- Olsen, A., Konovalov, D.A., Philippa, B., Ridd, P., Wood, J.C., Johns, J., Banks, W., Girgenti, B., Kenny, O., Whinney, J., et al.: Deepweeds: A multiclass weed species image dataset for deep learning. *Scientific reports* 9(1), 2058 (2019) [1](#), [9](#)
- Sandberg, M., Ghidini, S., Alban, L., Dondona, A.C., Blagojevic, B., Bouwknecht, M., Lipman, L., Dam, J.S., Nastasijevic, I., Antic, D.: Applications of computer vision systems for meat safety assurance in abattoirs: A systematic review. *Food Control* p. 109768 (2023) [1](#)
- Khellaf, A., Lando, L., Trinh, Q.: 159p classical computer vision and modern deep-learning of pancreatic stroma histology features to diagnose cancer. *Annals of Oncology* 34, S1537 (2023) [1](#)
- Fooladgar, F., Nguyen Nhat to, M., Javadi, G., Sojoudi, S., Eshumani, W., Chang, S., Black, P., Mousavi, P., Abolmaesumi, P.: Semi-supervised learning from coarse histopathology labels. *Computer Methods in Biomechanics and Biomedical Engineering: Imaging & Visualization* 11(4), 1143–1150 (2023) [2](#)
- Van Engelen, J.E., Hoos, H.H.: A survey on semi-supervised learning. *Machine learning* 109(2), 373–440 (2020) [2](#), [3](#)
- Zimmerer, D., Full, P.M., Isensee, F., Jäger, P., Adler, T., Petersen, J., Köhler, G., Ross, T., Reinke, A., Kascenas, A., et al.: Mood 2020: A public benchmark for out-of-distribution detection and localization on medical images. *IEEE Transactions on Medical Imaging* 41(10), 2728–2738 (2022) [2](#)
- Yang, J., Wang, P., Zou, D., Zhou, Z., Ding, K., Peng, W., Wang, H., Chen, G., Li, B., Sun, Y., et al.: Openood: Benchmarking generalized out-of-distribution detection. *Advances in Neural Information Processing Systems* 35, 32598–32611 (2022) [2](#), [3](#), [9](#), [11](#), [13](#)
- Assran, M., Caron, M., Misra, I., Bojanowski, P., Joulin, A., Ballas, N., Rabbat, M.: Semi-supervised learning of visual features by non-parametrically predicting view assignments with support samples. In: *Proceedings of the IEEE/CVF International Conference on Computer Vision*. pp. 8443–8452 (2021) [2](#), [4](#), [5](#), [6](#), [8](#), [9](#), [10](#), [11](#), [13](#), [26](#)
- Ming, Y., Sun, Y., Dia, O., Li, Y.: How to exploit hyperspherical embeddings for out-of-distribution detection? *arXiv preprint arXiv:2203.04450* (2022) [2](#), [3](#), [11](#), [13](#)
- Lu, H., Gong, D., Wang, S., Xue, J., Yao, L., Moore, K.: Learning with mixture of prototypes for out-of-distribution detection. In: *The Twelfth International Conference on Learning Representations* (2024), <https://openreview.net/forum?id=uNkKaD3MCs> [2](#), [3](#), [11](#), [13](#)

11. Bai, H., Ming, Y., Katz-Samuels, J., Li, Y.: Provable out-of-distribution generalization in hypersphere. In: The Twelfth International Conference on Learning Representations (2024), <https://openreview.net/forum?id=VXak3CZZGC> 2
12. Yang, H.M., Zhang, X.Y., Yin, F., Liu, C.L.: Robust classification with convolutional prototype learning. In: Proceedings of the IEEE conference on computer vision and pattern recognition. pp. 3474–3482 (2018) 2
13. Snell, J., Swersky, K., Zemel, R.: Prototypical networks for few-shot learning. *Advances in neural information processing systems* 30 (2017) 2
14. Radford, A., Kim, J.W., Hallacy, C., Ramesh, A., Goh, G., Agarwal, S., Sastry, G., Askell, A., Mishkin, P., Clark, J., et al.: Learning transferable visual models from natural language supervision. In: International conference on machine learning. pp. 8748–8763. PMLR (2021) 2, 3, 9, 26
15. Chen, T., Kornblith, S., Norouzi, M., Hinton, G.: A simple framework for contrastive learning of visual representations. In: International conference on machine learning. pp. 1597–1607. PMLR (2020) 2
16. Zhou, C., Li, Q., Li, C., Yu, J., Liu, Y., Wang, G., Zhang, K., Ji, C., Yan, Q., He, L., et al.: A comprehensive survey on pretrained foundation models: A history from bert to chatgpt. arXiv preprint arXiv:2302.09419 (2023) 2
17. Oquab, M., Darcet, T., Moutakanni, T., Vo, H., Szafraniec, M., Khalidov, V., Fernandez, P., Haziza, D., Massa, F., El-Nouby, A., et al.: Dinov2: Learning robust visual features without supervision. arXiv preprint arXiv:2304.07193 (2023) 2, 3, 9
18. Berthelot, D., Carlini, N., Goodfellow, I., Papernot, N., Oliver, A., Raffel, C.A.: Mixmatch: A holistic approach to semi-supervised learning. *Advances in neural information processing systems* 32 (2019) 2, 7
19. Rani, V., Nabi, S.T., Kumar, M., Mittal, A., Kumar, K.: Self-supervised learning: A succinct review. *Archives of Computational Methods in Engineering* 30(4), 2761–2775 (2023) 3
20. Cherti, M., Beaumont, R., Wightman, R., Wortsman, M., Ilharco, G., Gordon, C., Schuhmann, C., Schmidt, L., Jitsev, J.: Reproducible scaling laws for contrastive language-image learning. In: Proceedings of the IEEE/CVF Conference on Computer Vision and Pattern Recognition. pp. 2818–2829 (2023) 3
21. Lee, D.H., et al.: Pseudo-label: The simple and efficient semi-supervised learning method for deep neural networks. In: Workshop on challenges in representation learning, ICML. vol. 3, p. 896. Atlanta (2013) 3
22. Sohn, K., Berthelot, D., Carlini, N., Zhang, Z., Zhang, H., Raffel, C.A., Cubuk, E.D., Kurakin, A., Li, C.L.: Fixmatch: Simplifying semi-supervised learning with consistency and confidence. *Advances in neural information processing systems* 33, 596–608 (2020) 3, 4
23. Li, S., Jin, W., Wang, Z., Wu, F., Liu, Z., Tan, C., Li, S.Z.: Semireward: A general reward model for semi-supervised learning. arXiv preprint arXiv:2310.03013 (2023) 3, 10
24. Wang, Y., Chen, H., Heng, Q., Hou, W., Fan, Y., Wu, Z., Wang, J., Savvides, M., Shinozaki, T., Raj, B., et al.: Freematch: Self-adaptive thresholding for semi-supervised learning. In: The Eleventh International Conference on Learning Representations (2022) 3, 4, 10
25. Cai, Z., Ravichandran, A., Favaro, P., Wang, M., Modolo, D., Bhotika, R., Tu, Z., Soatto, S.: Semi-supervised vision transformers at scale. *Advances in Neural Information Processing Systems* 35, 25697–25710 (2022) 3, 10

26. Nguyen, A., Yosinski, J., Clune, J.: Deep neural networks are easily fooled: High confidence predictions for unrecognizable images. In: Proceedings of the IEEE conference on computer vision and pattern recognition. pp. 427–436 (2015) [3](#)
27. Tao, L., Du, X., Zhu, X., Li, Y.: Non-parametric outlier synthesis. arXiv preprint arXiv:2303.02966 (2023) [3](#)
28. Sun, Y., Ming, Y., Zhu, X., Li, Y.: Out-of-distribution detection with deep nearest neighbors. In: International Conference on Machine Learning. pp. 20827–20840. PMLR (2022) [3](#), [10](#), [11](#)
29. Lakshminarayanan, B., Pritzel, A., Blundell, C.: Simple and scalable predictive uncertainty estimation using deep ensembles. *Advances in neural information processing systems* 30 (2017) [3](#), [11](#)
30. Wei, H., Xie, R., Cheng, H., Feng, L., An, B., Li, Y.: Mitigating neural network overconfidence with logit normalization. In: International Conference on Machine Learning. pp. 23631–23644. PMLR (2022) [3](#), [11](#)
31. Hinton, G.E., Roweis, S.: Stochastic neighbor embedding. *Advances in neural information processing systems* 15 (2002) [3](#), [7](#)
32. Wang, Y., Huang, H., Rudin, C., Shaposhnik, Y.: Understanding how dimension reduction tools work: an empirical approach to deciphering t-sne, umap, trimap, and pacmap for data visualization. *The Journal of Machine Learning Research* 22(1), 9129–9201 (2021) [3](#)
33. Van der Maaten, L., Hinton, G.: Visualizing data using t-sne. *Journal of machine learning research* 9(11) (2008) [3](#), [8](#)
34. Wang, X., Lian, L., Yu, S.X.: Unsupervised selective labeling for more effective semi-supervised learning. In: European Conference on Computer Vision. pp. 427–445. Springer (2022) [4](#), [9](#), [12](#), [14](#), [26](#)
35. Chen, L., Bai, Y., Huang, S., Lu, Y., Wen, B., Yuille, A.L., Zhou, Z.: Making your first choice: To address cold start problem in vision active learning. arXiv preprint arXiv:2210.02442 (2022) [4](#)
36. Carlini, N., Erlingsson, U., Papernot, N.: Distribution density, tails, and outliers in machine learning: Metrics and applications. arXiv preprint arXiv:1910.13427 (2019) [4](#)
37. Caron, M., Misra, I., Mairal, J., Goyal, P., Bojanowski, P., Joulin, A.: Unsupervised learning of visual features by contrasting cluster assignments. *Advances in neural information processing systems* 33, 9912–9924 (2020) [4](#)
38. Chen, T., Kornblith, S., Swersky, K., Norouzi, M., Hinton, G.E.: Big self-supervised models are strong semi-supervised learners. *Advances in neural information processing systems* 33, 22243–22255 (2020) [4](#)
39. Mo, S., Su, J.C., Ma, C.Y., Assran, M., Misra, I., Yu, L., Bell, S.: Ropaws: Robust semi-supervised representation learning from uncurated data. arXiv preprint arXiv:2302.14483 (2023) [4](#), [7](#), [14](#), [22](#), [23](#)
40. Watson, G.S.: Distributions on the circle and sphere. *Journal of Applied Probability* 19(A), 265–280 (1982) [7](#)
41. Govindarajan, H., Sidén, P., Roll, J., Lindsten, F.: Dino as a von mises-fisher mixture model. In: The Eleventh International Conference on Learning Representations (2022) [7](#)
42. Van Der Maaten, L.: Learning a parametric embedding by preserving local structure. In: Artificial intelligence and statistics. pp. 384–391. PMLR (2009) [8](#)
43. Wang, M., Wang, D.: Vmf-sne: Embedding for spherical data. In: 2016 IEEE International Conference on Acoustics, Speech and Signal Processing (ICASSP). pp. 2344–2348. IEEE (2016) [8](#)

44. Lloyd, S.: Least squares quantization in pcm. *IEEE transactions on information theory* 28(2), 129–137 (1982) [9](#)
45. Krizhevsky, A., Hinton, G., et al.: Learning multiple layers of features from tiny images (2009) [9](#)
46. Helber, P., Bischke, B., Dengel, A., Borth, D.: Eurosat: A novel dataset and deep learning benchmark for land use and land cover classification. *IEEE Journal of Selected Topics in Applied Earth Observations and Remote Sensing* 12(7), 2217–2226 (2019) [9](#)
47. Nilsback, M.E., Zisserman, A.: Automated flower classification over a large number of classes. In: 2008 Sixth Indian conference on computer vision, graphics & image processing. pp. 722–729. *IEEE* (2008) [9](#)
48. Bossard, L., Guillaumin, M., Van Gool, L.: Food-101—mining discriminative components with random forests. In: *Computer Vision—ECCV 2014: 13th European Conference, Zurich, Switzerland, September 6–12, 2014, Proceedings, Part VI* 13. pp. 446–461. *Springer* (2014) [9](#)
49. Parkhi, O.M., Vedaldi, A., Zisserman, A., Jawahar, C.: Cats and dogs. In: 2012 IEEE conference on computer vision and pattern recognition. pp. 3498–3505. *IEEE* (2012) [9](#)
50. Le, Y., Yang, X.: Tiny imagenet visual recognition challenge. *CS 231N* 7(7), 3 (2015) [10](#)
51. Zhou, B., Lapedriza, A., Khosla, A., Oliva, A., Torralba, A.: Places: A 10 million image database for scene recognition. *IEEE transactions on pattern analysis and machine intelligence* 40(6), 1452–1464 (2017) [10](#)
52. Cimpoi, M., Maji, S., Kokkinos, I., Mohamed, S., Vedaldi, A.: Describing textures in the wild. In: *Proceedings of the IEEE Conf. on Computer Vision and Pattern Recognition (CVPR)* (2014) [10](#)
53. Deng, L.: The mnist database of handwritten digit images for machine learning research [best of the web]. *IEEE signal processing magazine* 29(6), 141–142 (2012) [10](#)
54. Netzer, Y., Wang, T., Coates, A., Bissacco, A., Wu, B., Ng, A.Y.: Reading digits in natural images with unsupervised feature learning (2011) [10](#)
55. Yang, L., Zhao, Z., Qi, L., Qiao, Y., Shi, Y., Zhao, H.: Shrinking class space for enhanced certainty in semi-supervised learning. In: *Proceedings of the IEEE/CVF International Conference on Computer Vision*. pp. 16187–16196 (2023) [10](#)
56. Hendrycks, D., Zou, A., Mazeika, M., Tang, L., Li, B., Song, D., Steinhardt, J.: Pixmix: Dreamlike pictures comprehensively improve safety measures. In: *Proceedings of the IEEE/CVF Conference on Computer Vision and Pattern Recognition*. pp. 16783–16792 (2022) [11](#)
57. Sehwal, V., Chiang, M., Mittal, P.: Ssd: A unified framework for self-supervised outlier detection. *arXiv preprint arXiv:2103.12051* (2021) [11](#)
58. Zhou, B., Zhao, H., Puig, X., Fidler, S., Barriuso, A., Torralba, A.: Scene parsing through ade20k dataset. In: *Proceedings of the IEEE conference on computer vision and pattern recognition*. pp. 633–641 (2017) [21](#)
59. Wu, Z., Xiong, Y., Yu, S.X., Lin, D.: Unsupervised feature learning via non-parametric instance discrimination. In: *Proceedings of the IEEE conference on computer vision and pattern recognition*. pp. 3733–3742 (2018) [24](#)
60. Paszke, A., Gross, S., Massa, F., Lerer, A., Bradbury, J., Chanan, G., Killeen, T., Lin, Z., Gimelshein, N., Antiga, L., Desmaison, A., Kopf, A., Yang, E., DeVito, Z., Raison, M., Tejani, A., Chilamkurthy, S., Steiner, B., Fang, L., Bai, J., Chintala, S.: PyTorch: An Imperative Style, High-Performance Deep Learning Library. In:

- Wallach, H., Larochelle, H., Beygelzimer, A., d'Alché Buc, F., Fox, E., Garnett, R. (eds.) Advances in Neural Information Processing Systems 32. pp. 8024–8035. Curran Associates, Inc. (2019), <http://papers.neurips.cc/paper/9015-pytorch-an-imperative-style-high-performance-deep-learning-library.pdf> 26
61. Falcon, W., The PyTorch Lightning team: PyTorch Lightning (Mar 2019), <https://github.com/Lightning-AI/lightning> 26
62. Yadan, O.: Hydra - a framework for elegantly configuring complex applications. Github (2019), <https://github.com/facebookresearch/hydra> 26
63. Raschka, S., Patterson, J., Nolet, C.: Machine learning in python: Main developments and technology trends in data science, machine learning, and artificial intelligence. arXiv preprint arXiv:2002.04803 (2020) 26

Supplementary Material

A Additional results

Consistency based loss can degrade the performance of PAWS during a training run. In Fig. S1 the training curves for two of the datasets from Fig. 3 in the paper are shown. These training curves demonstrate that the consistency loss can result in performance degrading for CIFAR-10 after around 10 epochs. When using the mixmatch loss, the validation accuracy remains stable once the models have converged. It is also noted that the performance improvement from vMF-SNE pretraining is not due to a head-start in training. While it does provide a better starting point for learning, in both cases models are trained until they completely converge, and vMF-SNE pretrained projection heads converge to higher performing maxima, particularly for the DeepWeeds dataset where training using a randomly initialised projection head leads to poor performance.

SKMPS selects a more diverse sample than USL. In Fig. S2 we compare diversity of classes sampled for the USL and SKMPS strategies for progressively larger budgets for CIFAR-10, CIFAR-100 and Food-101 datasets. In all three cases, the SKMPS strategy samples a greater diversity of images, as measured by the number of classes sampled from each dataset for a given budget. When not all classes are sampled, this reduces the maximum attainable performance for a model as classes that are not represented by atleast one labelled image cannot be learned in the PAWS framework.

The PAWS-VMK projection head provides more reliable OOD detection than the backbone embedding. In Tab. S1 and Tab. S2 we present the full set of results for each dataset in the OpenOOD benchmark. We also provide results for the backbone embedding and compare them to the PAWS and PAWS-VMK projection heads. For the backbone approach, we select prototypes using the SKMPS strategy and use the smallest cosine distance to a prototype

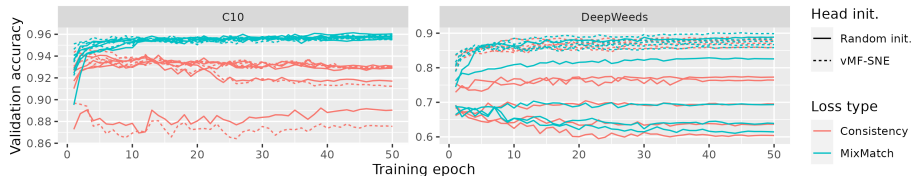
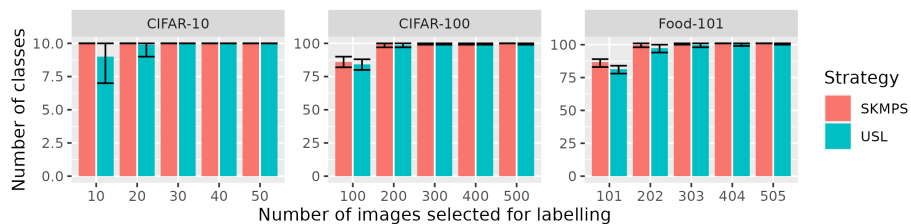
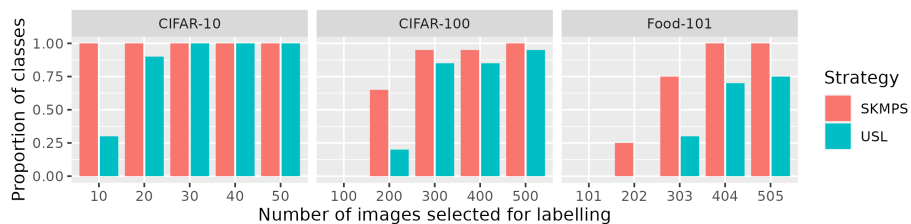


Fig. S1: Training curves comparing the vMF-SNE and random initialisation of the projection head and consistency versus mixmatch loss.



(a) Average number of classes sampled over 20 runs. Error bars show maximum and minimum number of classes sampled.



(b) Proportion of sets sampling all classes over 20 runs.

Fig. S2: Class diversity captured by different prototype selection strategies.

as our OOD metric, as done previously. In general we find that the backbone embedding performs better on the datasets that are included in the DINOv2 training set, such as ImageNet, DTD and Places365 (which is included in the ADE20K dataset [58]). However, the backbone performs very poorly on datasets it hasn't seen before such as CIFAR-10, CIFAR-100, MNIST and SVHN, while our projection heads, particularly the PAWS-VMK embeddings, can still perform well. Overall, the backbone performs slightly better on the near OOD CIFAR-10 benchmark (+0.82), while the PAWS-VMK embeddings outperforms on the far OOD CIFAR-10 (+3.31) and both CIFAR-100 (+6.87/+7.10) benchmarks.

Projection heads pretrained using the vMF-SNE approach perform better than random initialisation, even if they are pretrained using a different dataset. In (Tab. S3) we fit models on the DeepWeeds dataset randomly initialising the projection head, and then use projection heads pretrained on various datasets using our vMF-SNE approach. We found that pretraining the projection head is better than random initialisation in every case, but best performance was obtained when pretraining was undertaken on DeepWeeds. Potentially, our vMF-SNE approach could be used as a self-supervised method to pretrain a projection head for a foundational model on a large dataset, and this could then be used to obtain better performance than random initialisation on smaller datasets.

vMF-SNE and MixMatch loss also provide performance improvements when used with RoPAWS. It is shown in Tab. S4 that our approach also im-

Table S1: Detection performance on near OOD datasets with the DINOv2 ViT-S/14 frozen backbone. The \uparrow means larger values are better and the \downarrow means smaller values are better. **Bolded** numbers indicate the best result for a particular dataset. The left-most column indicates the in-distribution-dataset (IDD).

IDD	Method	Near OOD Datasets						Average	
		CIFAR-10		CIFAR-100		Tiny ImageNet		AUROC \uparrow	FPR \downarrow
		AUROC \uparrow	FPR \downarrow	AUROC \uparrow	FPR \downarrow	AUROC \uparrow	FPR \downarrow		
CIFAR-100	PAWS	90.11	51.13			90.99	46.54	90.55	48.84
	PAWS-VMK	95.79	26.05			94.60	32.30	95.19	29.18
	<i>backbone</i>	85.51	60.16			91.13	30.6	88.32	45.38
CIFAR-10	PAWS			82.10	73.90	83.19	69.49	82.64	71.70
	+mixmatch			91.61	43.36	91.12	42.78	91.37	43.07
	+vMF-SNE			92.84	40.43	93.50	34.92	93.17	37.68
	PAWS-VMK			93.34	35.94	92.83	33.30	93.09	34.62
	<i>backbone</i>			90.66	40.13	97.16	11.12	93.91	25.62

proves the performance obtained when training RoPAWS [39] on in-distribution data. This suggests that the characteristics of PAWS that leads to poor performance on DeepWeeds and CIFAR-10 when training with a frozen DINOv2 foundation model as a backbone also hold for RoPAWS.

Table S2: Detection performance on far OOD datasets with the DINOv2 ViT-S/14 frozen backbone. The \uparrow means larger values are better and the \downarrow means smaller values are better. **Bolded** numbers indicate the best result for a particular dataset. The left-most column indicates the in-distribution-dataset (IDD).

IDD	Method	Far OOD Datasets								Average	
		DTD		MNIST		SVHN		Places365		AUROC \uparrow	FPR \downarrow
		AUROC \uparrow	FPR \downarrow	AUROC \uparrow	FPR \downarrow	AUROC \uparrow	FPR \downarrow	AUROC \uparrow	FPR \downarrow		
CIFAR-100	PAWS	93.59	35.71	97.30	13.95	94.33	32.66	92.78	39.65	94.50	30.49
	PAWS-VMK	96.55	22.29	98.96	2.27	94.35	33.39	95.22	28.58	96.27	21.63
	<i>backbone</i>	98.92	4.8	87.98	86.15	72.76	85.57	97.03	12.18	89.17	47.18
CIFAR-10	PAWS	91.36	48.71	96.44	15.37	84.99	81.74	89.27	54.24	90.52	50.01
	+mixmatch	95.44	27.84	98.67	5.35	93.81	39.49	94.48	27.4	95.6	25.02
	+vMF-SNE	96.05	24.95	98.68	1.91	95.50	28.77	96.06	22.20	96.57	19.46
	PAWS-VMK	97.45	15.62	99.78	0.00	98.04	10.78	96.70	17.13	97.99	10.88
	<i>backbone</i>	99.96	0.16	99.4	1.91	80.57	71.18	98.8	4.17	94.68	19.36

Table S3: Transferability of vMF-SNE pretraining between datasets.

Method	Components			Dataset
	Head init.	Loss type	Label selection	
	Random init.	Mixmatch	Random stratified	76.0 \pm 9.3
	vMF-SNE pretrained on C100	Mixmatch	Random stratified	79.9 \pm 8.1
	vMF-SNE pretrained on C10	Mixmatch	Random stratified	81.5 \pm 7.1
	vMF-SNE pretrained on Food	Mixmatch	Random stratified	84.2 \pm 6.0
PAWS-VM	vMF-SNE pretrained on DeepWeeds	Mixmatch	Random stratified	87.8 \pm 1.5

Table S4: Compatability of our approach with RoPAWS.

Method	Components			Dataset	
	Head init.	Loss type	Label selection	C10	DeepWeeds
RoPAWS [39]	Random init.	RoPAWS-Consistency	Random stratified	93.3 \pm 1.5	81.2 \pm 6.8
RoPAWS-VM	vMF-SNE	RoPAWS-Mixmatch	Random stratified	95.7 \pm 0.1	86.4 \pm 0.6

B Additional results for vMF-SNE pretraining

B.1 Performance

Table S5: KNN accuracy of the model backbone versus the self-supervised vMF-SNE projection head. **Bolded** entries indicate the best results for a particular dataset.

Embedding	Dataset						
	C10	C100	EuroSAT	DeepWeeds	Flowers	Food	Pets
DINOv2 ViT-S/14 backbone	96.2	82.3	90.0	88.7	99.3	80.9	91.5
vMF-SNE proj. head	96.3±0.1	79.0±0.1	91.9±0.1	91.3±0.1	98.2±0.5	81.0±0.1	93.0±0.1

In a classification context, the performance of the backbone model can be measured non-parametrically using a weighted k-Nearest Neighbor (kNN) Classifier [59]. This provides for a quantitative approach to measure the performance of the projection head trained using vMF-SNE, as reproducing the local structure of the backbone model should provide similar kNN accuracy. We find that for five of the seven datasets considered, we can meet or beat the kNN accuracy of the backbone model through vMF-SNE pretraining (Tab. S5).

B.2 Hyperparameter ablation study

We undertook an ablation study to determine the sensitivity of vMF-SNE pretraining performance the hyper-parameters within the algorithm. It was found that the method was highly insensitive to most parameters for the CIFAR-10 dataset, with only a significantly lower perplexity γ or an order of magnitude higher concentration parameter τ resulting in changes to the kNN validation accuracy outside a single standard deviation (Tab. S6). The optimal parameter set appeared to be different between CIFAR-100 and the Food-101 datasets, with better performance for CIFAR-100 with a larger perplexity and smaller concentration and batch size, but better performance for Food-101 with a smaller perplexity and larger batch size. We also explored using a Gaussian kernel with CIFAR-10, and found that this resulted in much poorer performance.

Table S6: Ablation study on the vMF-SNE pretraining hyperparameters. The results for the parameters used in the other results in this paper are reported as the mean KNN accuracy and standard deviation of five runs, while the other cases report a single run.

Perplexity (γ)	C10	C100	Food
5	96.1	74.0	81.7
30	96.3±0.1	79.0±0.1	81.0±0.1
50	96.3	79.5	80.9
100	96.3	80.1	80.7
vMF concentration (τ)	C10	C100	Food
0.01	96.4	79.4	78.8
0.10	96.3±0.1	79.0±0.1	81.0±0.1
1.00	91.7	54.9	68.5
Z_2 dimension	C10	C100	Food
128	96.3	79.1	81.0
256	96.3	79.0	81.0
384	96.4	79.1	81.0
512	96.3±0.1	79.0±0.1	81.0±0.1
1024	96.3	79.0	81.0
Batch size	C10	C100	Food
128	96.2	79.5	80.4
256	96.3	79.1	80.7
512	96.3±0.1	79.0±0.1	81.0±0.1
1024	96.3	79.2	81.3
Kernel	C10	C100	Food
vMF	96.3±0.1		
Gaussian	91.4±0.6		

C Further implementation details

C.1 PAWS

We adapted the PAWS and RoPAWS PyTorch [60] implementation available at this [GitHub repository](#) to our own codebase using PyTorch-Lightning [61] and Hydra [62], which we ensured produced identical results. We employed the same samplers, optimizers, scheduler, augmentations, projection head architecture et cetera as described in [8]. The hyperparameters we selected are described in Appendix D.

C.2 vMF-SNE pretraining

We re-used the same augmentations, optimizer, scheduler and other details as for PAWS. The key difference is that the vMF-SNE pretraining approach only requires the unlabelled dataloader, compared to PAWS which requires both a labelled and unlabelled dataloader. This meant vMF-SNE pretraining was slightly faster. We note that when using image augmentations for this approach, we treat each augmented view independently.

C.3 k -means clustering and USL

We used the gpu-optimised k -means method available within cuML [63]. We save the normalised global class token from the DINOv2 model applied to each image of the dataset using the validation transformations, and run the k -means clustering method over this matrix. This method is extremely fast and can easily process millions of rows. We use the best clustering result from ten runs, and choose the number of clusters according to the number of prototypes we wish to select. To select the prototype from each cluster, we choose the image with the largest cosine similarity to the cluster centroid.

To reproduce the USL [34] approach, we used the code published by the authors on [GitHub](#). There are quite a few hyperparameters that are used within the USL method, so we selected the set that was used for ImageNet with CLIP [14], another foundation model based on the ViT architecture, for all of our experiments.

D Hyperparameters and further details

D.1 PAWS

We closely follow the hyperparameters suggested for PAWS for RoPAWS and use the same set for every dataset. These are summarised in the table below.

Hyperparameter	Value
Sampler parameters	
Labelled Sampler	Class-stratified
Labelled batchsize	320
Classes per batch	All*
Unlabelled Sampler	Random
Unlabelled batchsize	512
Optimiser parameters	
Optimizer	LARS SGD
Weight decay	1e-6
Momentum	0.9
Scheduler parameters	
LR schedule	Cos. anneal. w/ lin. warmup
Start LR	0.3
Maximum LR	6.4
Final LR	0.064
Epochs	50
Training augmentations	
Global crop size	224
Global crop scale	(0.14, 1.0)
Local crop size	98
Local crop scale	(0.05, 0.14)
Color distortion s	0.5
Blur probability	0.0
Color distortion (grayscale)	No
Color distortion (solarize)	Yes
Color distortion (equalize)	Yes
normalize (mean)	(0.485, 0.456, 0.406)
normalize (SD)	(0.229, 0.224, 0.225)
Training augmentations	Labelled

Continued on next page

Continued from previous page

Hyperparameter	Value
Global crops	2
Local crops	0
Training augmentations	Unlabelled
Global crops	2
Local crops	6
Validation augmentations	
Resize	256
Center crop	224
normalize (mean)	(0.485, 0.456, 0.406)
normalize (SD)	(0.229, 0.224, 0.225)
PAWS	
Label smoothing	0.1
Sharpening T	0.25
Temperature	0.1
Me-max	Yes
RoPAWS	
Prior temperature	0.1
Prior power	1.0
Label ratio	5.0
S-batchsize	32
U-batchsize	512
Projection head	
Input dimension	384**
Hidden dimension	384
Output dimension	512
Layers	3

*Except for Food-101 where 100 classes per batch were selected. **This is the size of the output global token from the DINOv2 ViT-S/14 distilled model.

D.2 vMF-SNE pretraining

We use the same parameters as above, with the following additions and changes.

Hyperparameter	Value
Continued on next page	

Continued from previous page

Hyperparameter	Value
Sampler parameters	
Labelled Sampler	None
Labelled batchsize	-
Unlabelled Sampler	Random
Unlabelled batchsize	512
vMF-SNE parameters	
vMF concentration (τ)	0.1
Perplexity (γ)	30
kNN evaluation parameters	
Nearest neighbours	200
Temperature	0.1